



E-ISSN: 2278-4136
P-ISSN: 2349-8234
JPP 2019; 8(4): 891-898
Received: 01-05-2019
Accepted: 03-06-2019

G Anuradha
Department of Physics,
Kunthavai Nachiyaar
Government Arts College for
Women, Thanjavur,
Tamil Nadu, India

R Manimekalai
Department of Physics,
AVVM Sri Pushpam College
(Autonomous), Poondi,
Thanjavur, Tamil Nadu, India

Antibacterial activity of green synthesized copper sulphate doped gold nano particles from the leaf extract of *Aegle marmelos* L.

G Anuradha and R Manimekalai

Abstract

Biosynthesis of nanoparticles is a valuable method and highly safe with low cost. Gold nanoparticles have an enormous medical application, in recent years. This study demonstrates an optimized biosynthesis for stable gold nanoparticles (AuNPs) from methanolic extract of *Aegle marmelos* leaves. The biosynthesized gold nanoparticles characterization using UV-Vis spectrophotometer, Zeta seizer, X-ray diffraction, TEM, and FTIR. UV-Vis spectra of gold nanoparticles showed maximum absorption peak at 549.10 nm. From the TEM images, the size of AuNPs was found to be about 38.2 ± 10.5 nm. The synergistic effect of biosynthesized AuNPs gave highest fold increase against *E. faecalis*, *K.pneumoniae* and *K.oxytoca* as standard antibiotics respectively.

Keywords: Gold nano particles, *Aegle marmelos*, FT-IR, UV Vis Spectra, TEM, SEM, XRD

Introduction

Nanostructures possess valuable and unique chemical, optical and mechanical properties which permit using it in medical therapeutics and diagnosis. Gold nanoparticles (AuNPs) have applications in microbiology, medicine, environmental sensing and biosensors [1]. Biosynthesis of AuNPs has more economic advantages than physicochemical methods which need complex and hi-tech instrumentation facilities, harsh chemicals also, biomedical application of Nanoparticles will be safe if these nanoparticles prepared only with biocompatible chemicals to minimize toxicity [2].

Today, nano metal particles, especially gold, have drawn the concentration of scientists because of their all-embracing application in the development of new technologies in the areas of electronics, chemistry, medicine and biotechnology at the nano scale [3-6]. Gold nano particles could also have many new applications in biology in the field of biosensors and DNA labeling [7, 8].

The Cu nano particles have attracted the researchers due to its function of industrial and medical areas. The biological property exposed by Cu nano particles are wound dressings and biotical properties [9, 10] antibacterial [11], industrial use for instance gas sensors, catalytic process, superconductors and solar cells [12-14]. Plant extracts or plant biomass could be a option to chemical and physical methods for the production of nanoparticles [15, 16].

Plant based synthesis is relatively fast, safe and light and also works under normal condition without the needs of high physical requirements [17]. *A. marmelos* commonly known as bael tree belongs to the Rutaceae family. It originates from India and grows in outer Himalayan and south Indian plateau regions. *A. marmelos* is an important medicinal plant with several ethanomedicinal applications in traditional and folk medicine systems. The different parts of *A. marmelos* are used for various remedial purposes such as for treatment of asthma, anaemia, fractures, therapeutic of wounds, inflamed joints, high blood pressure, jaundice, diarrhea, healthy mind and brain typhoid troubles for the period of pregnancy [18].

In this study, the synthesized gold nano particles doped copper sulphate from medicinal plant extract of *A. marmelos*. The ACAuNps were characterized by UV Visible spectra, FT-IR, SEM, XRD, TEM and their biological activities

2. Materials and Methods:

The *A. marmelos* leaves were collected from the Big temple (Pragtheeswarar temple) in Thanjavur, Tamilnadu. The chloroauric acid (HAuCl_4), copper sulphate were purchased from Hi media, Mumbai. The bacterial pathogenic strains used in this study purchased from MTCC (Microbial Type Culture Collection), CSIR-Institute of Microbial Technology, Chandigarh, India.

Correspondence

G Anuradha
Department of Physics,
Kunthavai Nachiyaar
Government Arts College for
Women, Thanjavur,
Tamil Nadu, India

3. Experimental procedure

3.1 Green synthesis of optimized gold nano particles

The fresh leaves of *A. marmelos* were washed thoroughly with distilled water. The leaves were kept for drying in shade region and then finely powdered. The 25 g of *A. marmelos* leaf powder was mixed with 100 mL methanol. After 72 hours resultant extract was filtered with whatman filter paper, then plant extract (20 mL) was added to 2M aqueous solution of chloroauric acid (HAuCl_4) with continuous stirring. After that 1M aqueous solution of copper sulphate was added and the mixer solution was allowed to 3 hours 60°C for gentle stirring. The appearance of a purple colour in the reaction vessels confirmed the formation of gold nano particles. The ACAuNPs thus obtained were confirmed for further analysis.

3.2 Characterization of gold nano particles

The Synthesized ACAuNps were characterized by different techniques like FT-IR, UV-Visible spectra, SEM, TEM and XRD. UV-Vis Spectroscopy. Absorption spectra, in the range of 400–700nm, were obtained with a Thermo Genesys 10S spectrometer using a 1cm quartz cuvette. The Conjugates were measured by UV-Vis analysis to monitor the ACAuNps, Particle Size of ACAuNps functionalized to UBI were measured ($n=5$) using a particle size (dynamic light scattering). The FT-IR spectra of lyophilized samples were acquired on a Perkin Elmer System 2000 spectrometer with an ATR platform (Pike Technologies) by applying Attenuated Total Reflection Fourier Transform Infrared (ATR-FTIR) spectroscopy from 570 to 4400 cm^{-1} .

X-ray diffraction (XRD) measurement were carried out by Rigaku X-ray diffractometer (ULTIMA IV, Rigaku, Japan) with $\text{CuK}\alpha$ X-ray source ($\lambda=1.54056\text{\AA}$). The ACAuNps were characterized morphologically by SEM and TEM micrographs. The morphology of the ACAuNps nanoparticles was characterized using transmission electron microscopy (TEM) and scanning electron microscopy (SEM). For the TEM images a JEOL microscope model JEM-1011 HR was used. SEM images were recorded in the JEOL JSM-820 scanning electron microscope model Quanta 200 with field emission gun.

3.3 Antimicrobial assay

The antibacterial activity (Balan *et al.*, 2016) of the copper sulphate doped gold nano particles was tested against pathogenic bacterial strains by the micro dilution method in well flat-bottom plastic tissue culture plates (Biotek Elx808, WI, USA). They were *Streptococcus mutans* MTCC 890, *Staphylococcus aureus* MTCC 96, *Escherichia coli* MTCC 443, *Salmonella typhi* MTCC 733, *Vibrio parahaemolyticus* MTCC 451, *Bacillus subtilis* MTCC 619, *Micrococcus luteus*

MTCC 3911, *Enterococcus faecalis* MTCC 6845, *Klebsiella pneumoniae* MTCC 7162 and *Klebsiella oxytoca* MTCC 3030. For culture conditions, nutrient broth medium with pH 7 at 37°C temperature was used; briefly, 125 μL of sterile, double-strength culture medium were placed into the first column of the 96-well microtitre plates and 125 μL of sterile, single-strength culture medium in the remaining wells. Subsequently, 125 μL of stock solution in phosphate buffer saline at a 3200 $\mu\text{g}/\text{mL}$ concentration (PBS: 10 mM $\text{KH}_2\text{PO}_4/\text{K}_2\text{HPO}_4$ and 150mM NaCl with pH adjusted to 7.0) were added to the first column of the microtitre plates and mixed with the medium; this results in a stock concentration of 400 $\mu\text{g}/\text{mL}$; serially, 125 μL were transferred to the subsequent wells, discarding 125 μL of the mixture in the tenth column, so that the final volume for each well was 125 μL .

This process results in two fold serial dilutions of the stock substance concentration in the first 10 columns (400– 780 $\mu\text{g}/\text{mL}$). Columns 11 and 12 did not contain test substances and served as negative and growth controls, respectively. All the wells (except for the 11th column) were inoculated with 2.5 μL of an overnight culture at the defined optimum conditions, diluted to 10^8 cfu/mL. Microtitre plates were covered and incubated for 48 h under the appropriate growth conditions for each bacteria. Triplicate assays were performed for all test concentrations used for each zone. After 48 h of incubation, the absorbance at 600 nm was determined for zone.

3.4 Confocal laser scanning microscopy (CLSM)

The antibacterial activity of the ACAuNPs synthesized from *A. marmelos* tested against pathogenic bacterial strains visualized with the help of CLSM which revealed the density of viable pathogenic cells after the treatment. After 48 h incubation, bacterial smear from 20 μL (microdilution method) was prepared from the individual positive microtitre plates on glass microscopic slides and fixed with 2% (v/v) glutaraldehyde in phosphate-buffered saline (PBS), pH 7.4 (137 mM NaCl, 3 mM KCl, 10 mM Na_2HPO_4 , and 2mM KH_2PO_4), for 15min. Excess fixative was removed by washing the films with PBS for 15min. The bacterial smear were then stained with 0.01% (w/v) acridine orange (Sigma Chemicals, USA) in PBS for 15min, which was followed by washing with PBS for 30min to remove excess stain. The stained bacterial smear was visualized by CLSM with an Olympus LSMGB200 CLSM (Olympus Optical Co. Ltd., Tokyo, Japan). The CLSM used an argon ion laser at 488 nm for excitation and a 605–632 nm band-pass filter for emission. Images were captured and processed using Olympus LSMGB200 CLSM bundled programs (Rice *et al.*, 2005)

4. Results and discussion

4.1 FT-IR spectral analysis

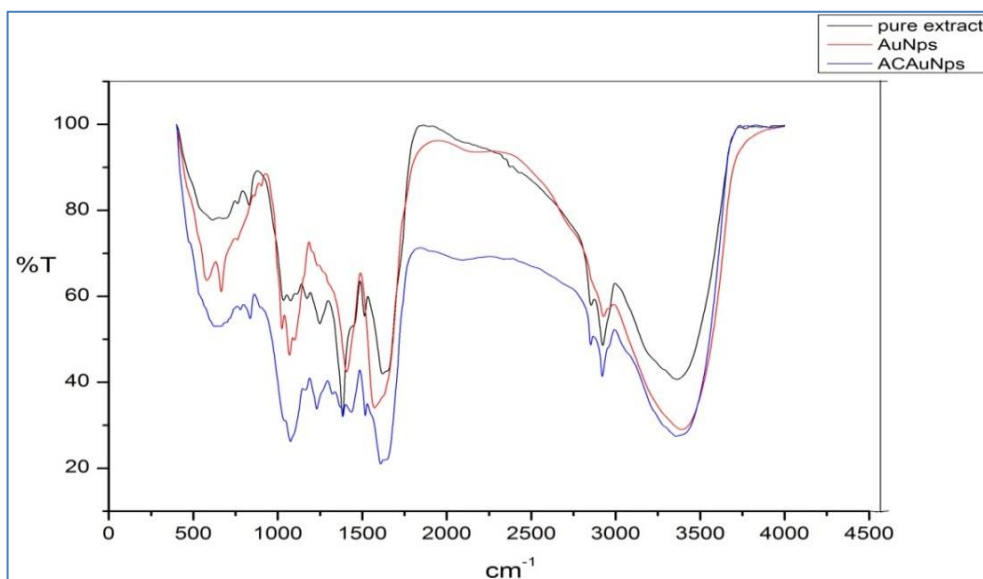


Fig 1: FT-IR Spectrum of green synthesized ACAuNPs

The plant having a bunch of bio-chemical molecules like stigmasterol, ergosterol and flavonoids play an significant role in synthesis and stabilizing of gold nano particles [20, 21]. These *A. marmelos* may actively involved in the reduction of gold ions to gold nano particles was characterized by FT-IR spectrum of leaf extract before and after reduction process. The bond at 3357.58 cm^{-1} corresponds to O-H stretching, 2920.75 cm^{-1} bond corresponds to C-H stretching of alcohol and phenols, 2852.14 cm^{-1} corresponds to C-H bond in

Xanthone [22]. The peaks at 1384.97 cm^{-1} and 1436.53 cm^{-1} presence of the O-H and C-N bond of polyphenol, confirm the presence of an aromatic group [23]. These observations bonds serrated in the region of 1000-1500 cm^{-1} are assigned to C=O stretching vibrations of organic phases surrounding the ACAuNps.

4.2 FT-IR spectra analysis

Table 1: FT-IR spectral data of ACAuNps

Wave numbers (cm^{-1})	Vibration modes
3357.58 cm^{-1}	O-H stretching
2920.75 cm^{-1}	C-H stretching
2852.24 cm^{-1}	C-H stretching
1608.85 cm^{-1}	H-O-H bonded
1436.53 cm^{-1}	C-N stretching aromatic amine
1384.97 cm^{-1}	O-H stretching
1000-1500 cm^{-1}	C=O bonded

The FT-IR spectrum results showed the absorption bands appeared at 3357.58 and 1384.97 cm^{-1} indicates ν O-H, 2920.75 and 2852.24 cm^{-1} indicates ν C-H, 1608.85 cm^{-1} indicates ν H-O-H, 1436.53 cm^{-1} indicates ν C-N and 1000-1500 cm^{-1} indicates ν C=O vibrational modes. The shifted

peaks clearly indicates that the formation of nano particles of methanolic extract of *A. marmelos*.

4.3 UV-Vis spectral analysis

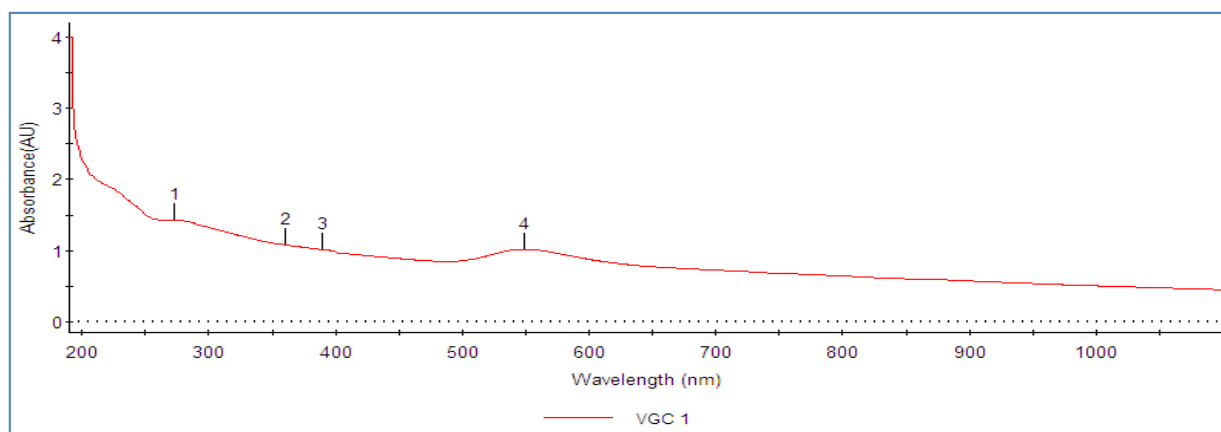


Fig 2: a) UV-vis absorption spectra of gold nano particles

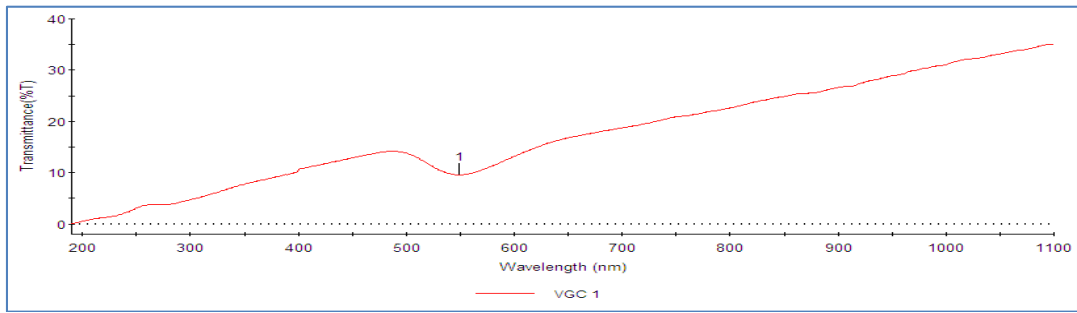


Fig 2: b) UV-vis transmittance spectra of ACAuNPs.

The presence of ACAuNPs is confirmed by a Sharp peak appears 549.10 nm of UV-vis spectrum. It is further confirmed by other characterizations that this peak indicated the formation of nano dispersed spherical shape ACAuNPs in the visible region of the electromagnetic spectrum. The colour

of the solution is also changed indicating the generation of ACAuNPs.

4.4 SEM and TEM analysis

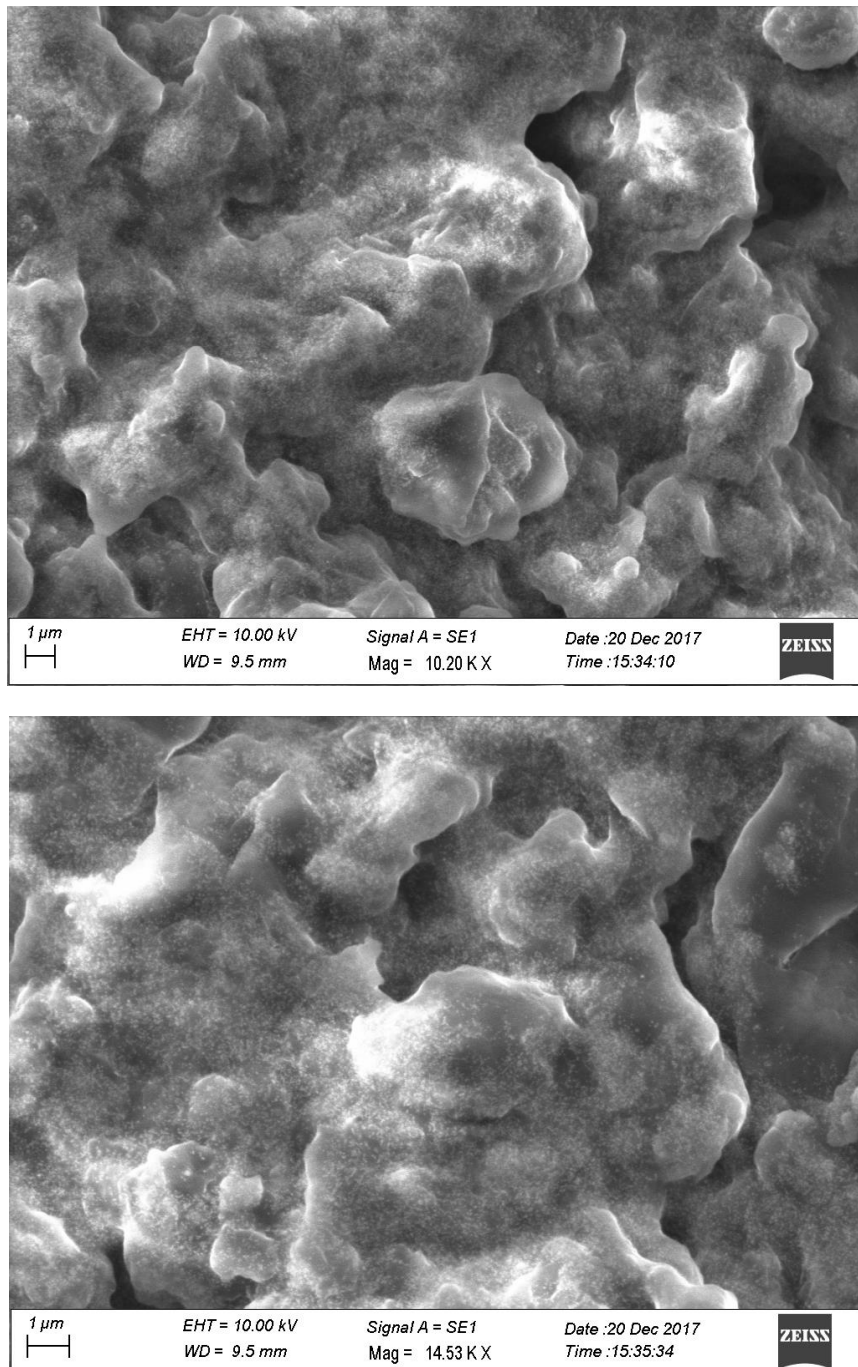


Fig 3: SEM images of gold nano particles

The surface morphology of the synthesized ACAuNPs was studied by SEM. The results obtained from SEM showed that the nano particles are crystalline in nature.

A TEM study reveals the size and shapes of nano particles. The shape of gold nano particles prepared in this study is

spherical with size in the average diameter range of $\pm 5\text{nm}$. The size of the copper Nps using *A. marmelos* was 48nm (24) and the size of AuNps using *A. marmelos* was $38.2\pm 10.5\text{nm}$ (25) indicated the nano particles.

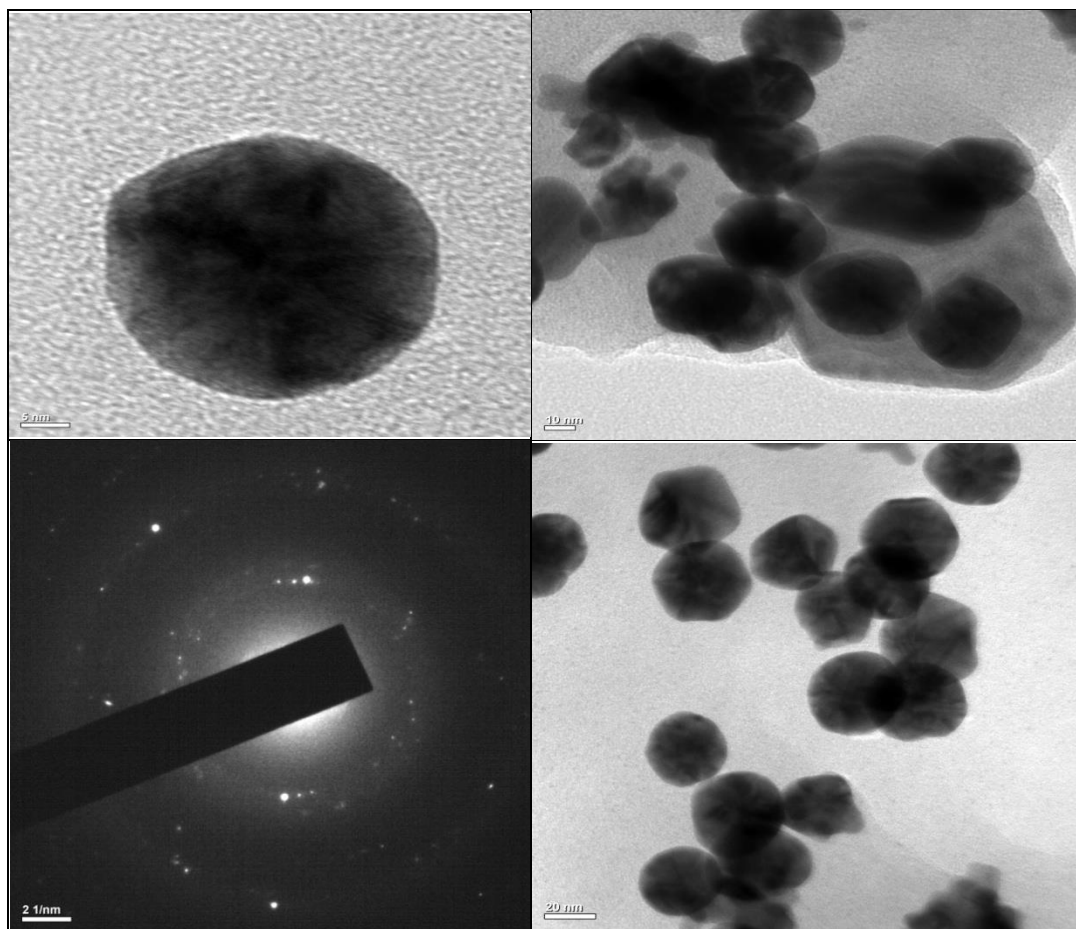


Fig 4: TEM images of gold nano particles

4.5 X-Ray diffraction Analysis

Structural characterization has been performed using XRD analysis and the typical XRD pattern of gold nano particles was shown. In addition to these three peaks there are some unidentified peaks appeared in the XRD pattern. The

characteristic peaks corresponding to (111) and (200) (220) and (311) of Au are located at $2\theta=38.22$, 44.45 , 64.77 and 77.97 respectively. The result indicates that the sample is composed of crystalline gold.

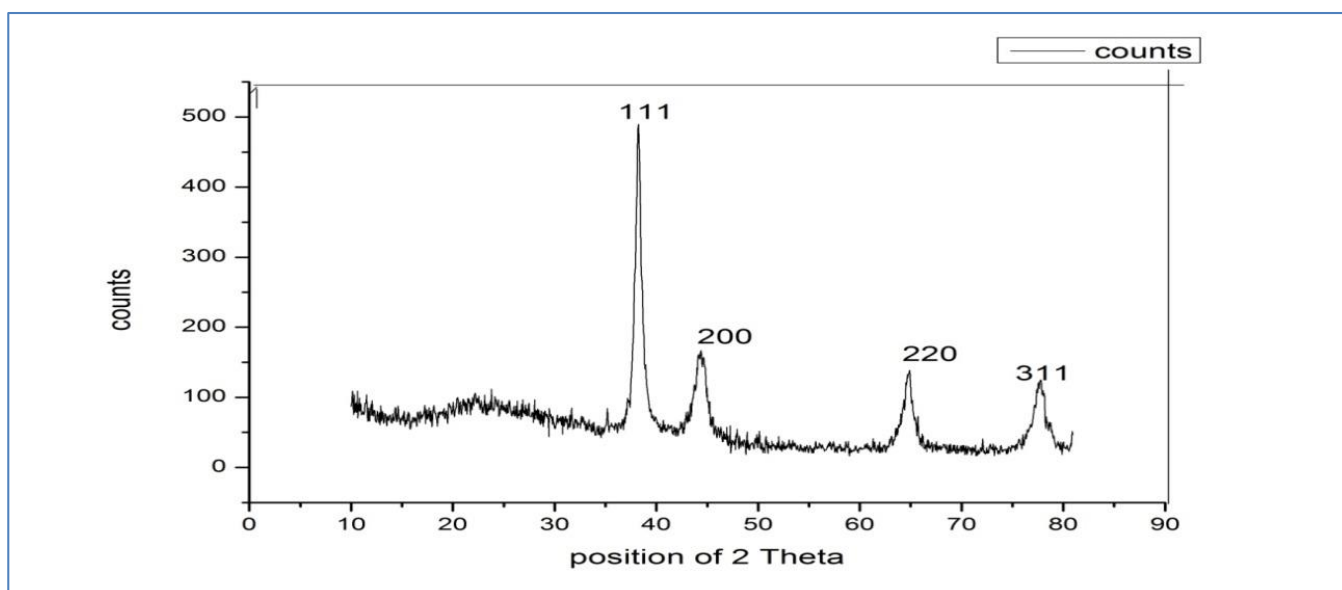
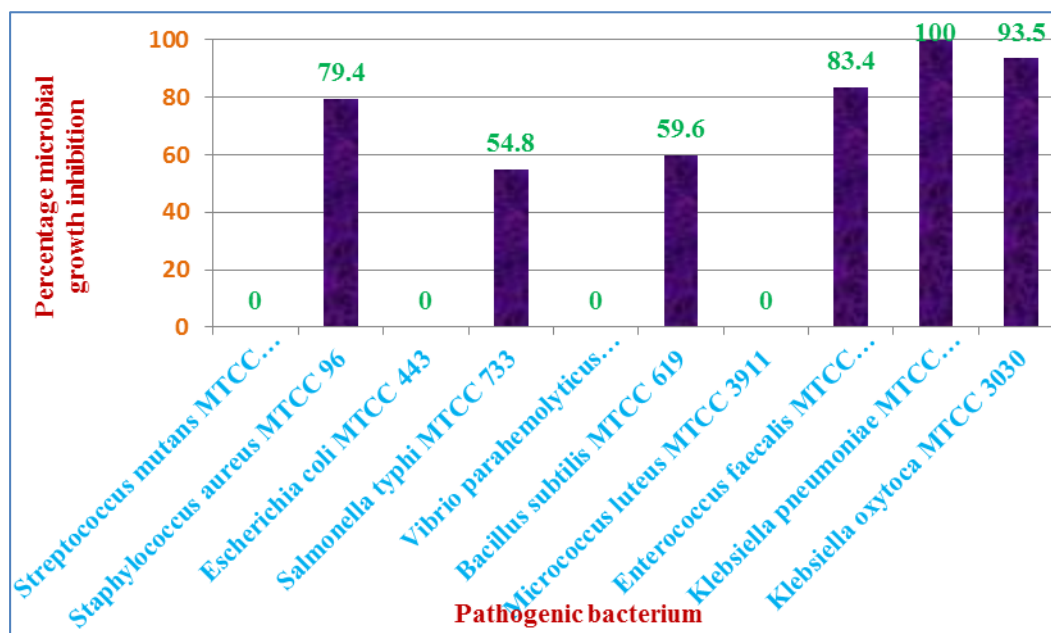
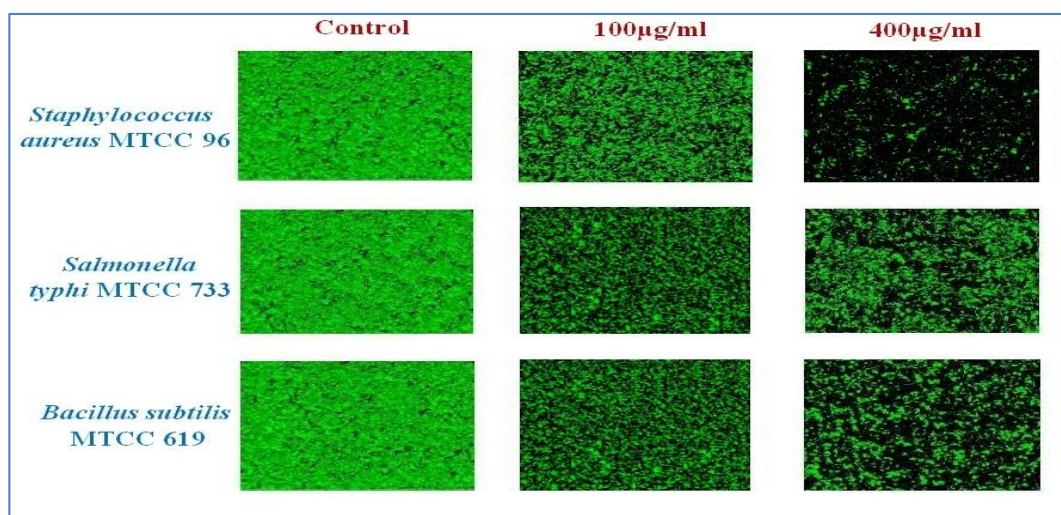


Fig 5: XRD pattern of synthesized ACAuNps

Table 2: Microbial growth inhibition percentages of ACAuNPs against various pathogenic bacteria at different concentrations

Name of the bacteria	Percentage of inhibition (%)					
	12.5 μ L	25 μ L	50 μ L	100 μ L	200 μ L	400 μ L
<i>S. mutans</i>	-	-	-	-	-	-
<i>S. aureus</i>	24.5 \pm 0.1	33.7 \pm 0.2	45.9 \pm 0.7	56.3 \pm 0.9	68.2 \pm 0.4	79.4 \pm 0.5
<i>E. coli</i>	-	-	-	-	-	-
<i>S. typhi</i>	7.5 \pm 0.2	16.8 \pm 0.4	29.1 \pm 0.5	39.4 \pm 0.7	41.7 \pm 0.6	54.8 \pm 0.8
<i>V. para hemolyticus</i>	-	-	-	-	-	-
<i>B. subtilis</i>	5.1 \pm 0.4	11.8 \pm 0.3	23.9 \pm 0.2	35.3 \pm 0.5	47.5 \pm 0.3	59.6 \pm 0.3
<i>M. luteus</i>	-	-	-	-	-	-
<i>E. faecalis</i>	23.6 \pm 0.5	35.3 \pm 0.3	46.2 \pm 0.7	59.8 \pm 0.6	71.5 \pm 0.1	83.4 \pm 0.8
<i>K. pneumoniae</i>	31.2 \pm 0.6	43.5 \pm 0.3	60.4 \pm 0.6	76.3 \pm 0.8	91.7 \pm 0.5	100 \pm 0.2
<i>K. oxytoca</i>	27.4 \pm 0.4	40.6 \pm 0.3	54.5 \pm 0.4	67.4 \pm 0.7	81.8 \pm 0.5	93.5 \pm 0.7

4.6 Graphical representation

**Fig 6:** Microbial growth inhibition percentages of ACAuNPs against various pathogenic bacteria at different concentrations**Fig 7:** Effect of different concentrations of ACAuNPs against *S. aureus*, *S. typhi* and *B. subtilis*

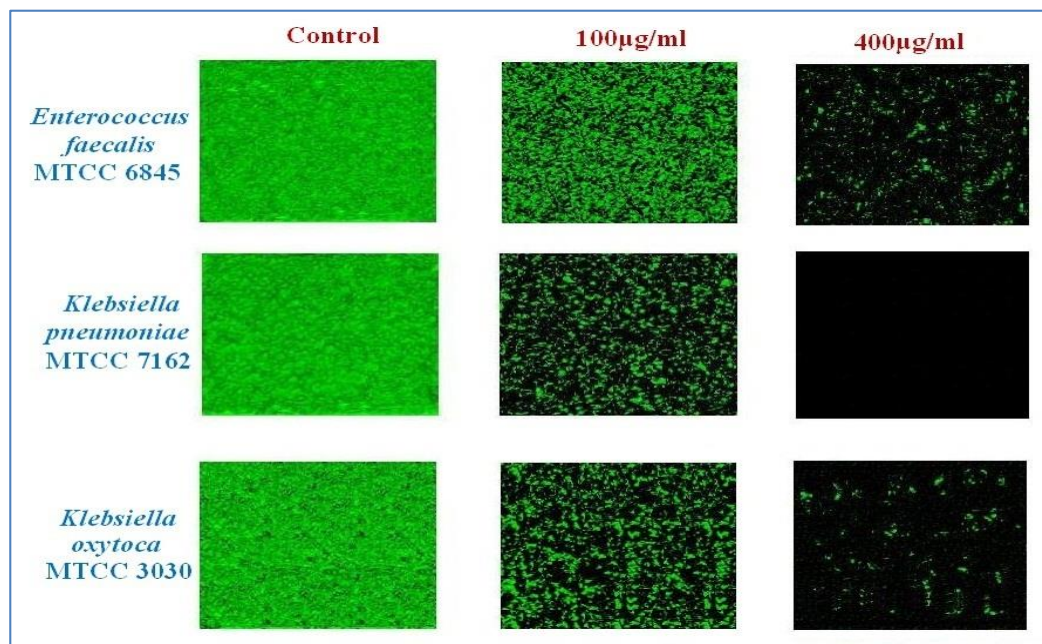


Fig 8: Effect of different concentrations of ACAuNPs against *E. faecalis*, *K. pneumoniae* and *K. oxytoca*.

In the present study the microbial growth inhibition percentages of ACAuNPs against *S. mutans*, *E. coli*, *V. parahemolyticus* and *M. luteus* were no % of inhibitions and other bacteria's such as *S. aureus*, *S. typhi*, *B. subtilis*, *E. faecalis*, *K. pneumoniae* and *K. oxytoca* were maximum % of inhibitions are at 400 µL. So increase in concentration increasing the % of inhibitions and maximum % of inhibitions were recorded on *K. pneumoniae* 100%, *K. oxytoca* 93.5%, *E. faecalis* 83.4%, *S. aureus* 79.4%, *B. subtilis* 59.6% and *S. typhi* 54.8% respectively. Thus the results indicated that ACAuNPs was also demonstrated in other studies mainly focused on bacteria showing resistance to conventional antibiotics. It is now clear that ACAuNPs possess a strong antibacterial activity, highlighted by several studies. Since ACAuNPs have the ability to interact with various microorganisms (such as bacteria) and also impact both the growth and mature bacterial pathogenic cells viable density.

5. Conclusion

In this study successfully biosynthesis of ACAuNPs from methanolic extract of *A. marmelos* leaves and was characterized by UV-Visible, XRD, TEM, and FTIR spectral techniques. The ACAuNPs was significant antibacterial activity. Thus, the as-synthesized CuO NPs proved the outstanding antibacterial efficacy, and it was well established by the clear zone of inhibitions against bacterial strains. Therefore, ACAuNPs could be used as broad spectrum of antimicrobials.

References

- Siddiqi KS, Husen A. Fabrication of metal nanoparticles from fungi and metal salts: Scope and application. Nano scale research letters. 2016; 11(1):98.
- Shedbalkar U, Singh R, Wadhvani S, Gaidhani S, Chopade BA. Microbial synthesis of gold nanoparticles: Current status and future prospects. Advances in colloid and interface science. 2014; 209:40-48.
- Armendariz V, Gardea-Torresdey JL, Jose-Yacamán M, Gonzalez J, Herrera I, Parsons JG. Proceedings of the conference on application of waste remediation technologies to agricultural contamination of water resources, Kansas City, Mo (USA), 2002.
- Magudapathy P, Gangopadhyay P, Panigrahi BKK, Nair KGM, Dhara S. Electrical transport studies of Ag nanoclusters embedded in glass matrix. Physics of Condensed Matter. 2001; 299:142-146.
- Joerger R, Klaus T, Granqvist CG. Functional biomimetic surface coatings. Adv. Mater. 2000; 12:407-409.
- Tanak K. Nanotechnology towards 21st Century. Thin Solid Film. 1999; 341:120-125.
- Kohler JM, Csaki A, Reichert J, Moller R, Straube W, Fritzsche W. Sens. Actuators B: Synthesis of gold and silver stabilized with glycol saminogly cans having distinctive biological activities. Bio macro molecules. 2001; 76:166-172.
- Schatz GC, Lazarides AA, Kelly KL, Jensen TR. Optical properties of metal properties aggregates important in biosensors. J Mol. Struct. (Theochem). 2000; 529:59-63.
- Borkow G, Gabbay J, Dardik R. Molecular mechanisms of enhanced wound healing by copper oxide-impregnated dressings. Wound. Repair Regen. 2010; 18:266-75.
- Borkow G, Zatzoff RC, Gabbay J. Reducing the risk of skin pathologies in diabetics by using copper impregnated socks. Med. Hypotheses. 2009; 73:883-6.
- Theivasanthi T, Alagar M. Studies of Copper Nanoparticles Effects on Micro-organisms. Annals of Biological Research. 2011; 2:368.
- Li Y Liang, J Tao Z. CuO particles and plates: Synthesis and gas sensor application. J Chen. Mater. Res. Bull. 2007; 43:2380.
- Carnes LC, Klabunde KJ. The catalytic methanol synthesis over nanoparticle metal oxide catalysts. J Mol. Catal. A. Chem. 2003; 194:227.
- Guo Z, Liang X, Pereira T, Scaffaro R, Hahn H. CuO nanoparticle filled vinyl-ester resin nanocomposites: Fabrication, characterization and property analysis. Compos. Sci. Tech. 2007; 67:2036.
- Vanaja M, Rajeshkumar S, Gnanajobitha G, Paulkumar K, Malarkodi C, Annadurai G. Kinetic study on green synthesis of silver nanoparticles using coleus aromaticus leaf extract. Adv. Appl. Sci. Res. 2013; 4(3):50-55.
- Gnanajobitha G, Rajeshkumar S, Kannan C, Annadurai G. Preparation and characterization of fruit-mediated

- silver nanoparticles using pomegranate extract and assessment of its antimicrobial activity. *J Environ. Nano technol.* 2013; 2(1):04-10.
17. Chung IM, Park I, Seung-Hyun K, Thiruvengadam M, Rajakumar G. Plant-mediated synthesis of silver nanoparticles: their characteristic properties and therapeutic applications, *Nano scale Research Letters.* 2016; 11(1):1-14.
 18. Sharma GN, Dubey SK, Sati N. Evaluation of germination power of *Aegle marmelos* seeds. *J Chem. Pharm. Res.* 2011; 3(1):732-736.
 19. Philip D, Unni C. Extracellular biosynthesis of gold and silver nanoparticles using *Ocimum sanctum* leaf. *Phys. E.* 2011; 43(7):1318-1322.
 20. Mohammed-Fayaz A, Girilal M, Venkatesan R, Kalaichelvan PT. Biosynthesis of anisotropic gold nanoparticles using *Maduca longifolia* extract and their potential in infrared absorption. *Colloid. Surf B: Bio interf.* 2011; 88(1):287-291.
 21. Shameli K, Ahmad MB, Shabanzadeh P. Effect of *Curcuma longa* tuber powder extract on size of silver nanoparticles prepared by green method, *Research on Chemical Intermediates.* 2014; 40(3):1313-1325.
 22. National review and coordination meeting on nanoscience and nanotechnology. 2014; 8(10):401-404.
 23. Rao KJ, Paria S. Green synthesis of silver nanoparticles from aqueous *Aegle marmelos* leaf extract. *Mater. Res. Bull.* 2013; 48:628-634.
 24. Kreibeg U, Vollmer M. Optical properties of metal clusters, Springer, Series, Springer, Berlin, 1995, 25.